ELSEVIER

Chemical Engineering Journal 135S (2008) S210–S218

Chemical Engineering Journal

www.elsevier.com/locate/cej

Toolkit for computational fluidic simulation and interactive parametrization of segmented flow based fluidic networks

Nils Gleichmann [a], Daniell Malsch [a], Mark Kielpinski [a], Wilhelm Rossak [b], Günter Mayer [a], Thomas Henkel [a,*]

[a] *Microsystems Division, Institute for Physical High Technology, P.O. Box 100239, 07702 Jena, Germany*
[b] *Friedrich-Schiller-University Jena, Department of Informatics, D-07743 Jena, Germany*

Abstract

This paper describes a computational approach for system modelling and model based design of microfluidic networks for processing of microsegmented sample streams and its application for modelling of the self-controlled 1:1 fusion of two independently generated sample streams. Liquid/liquid segmented flow based highly integrated lab-on-a-chip devices offer a powerful and versatile approach for high-throughput processing of linearly organized sample streams. Main objectives of this work are the application of principles of electronic design automation (EDA) to the model based design and parametrization of segmented flow based microfluidic networks. This approach will significantly increase the efficiency in development of highly integrated lab-on-a-chip devices for custom fluidic and microchemical protocols. That way, research and development of microchemical and screening applications will benefit from the promising microdroplet based approach of segmented flow. Our computational toolkit is based on a network of fluidic nodes, which are interconnected by virtual fluid pipes for the transfer of segment streams. The particular behaviour of a functional node may be given by user definable rules, which may be derived from experimental data and parameter studies of computational fluid dynamics (CFD) simulations of the functional element.

Keywords: Microfluidics; System modelling; Lab-on-a-chip; Liquid/liquid two phase flow; Segmented flow; Microreaction technology

1. Introduction

The application of liquid/liquid microsegmented flow to serial high-throughput microanalytical systems offers promising prospects for applications in clinical chemistry, pharmaceutical research, process diagnostics, and analytical chemistry. Sample volumes down to a few nanoliters may be processed in a reliable way. Individuality and integrity of these volumes may be retained during the complete diagnostic process making the approach favoured for analysis of individual microscaled objects like cells and microorganisms embedded in droplets. Microscopy and microspectral analytics offer powerful approaches for the analytical readout of droplet based assays. At present, these fluidic networks are commonly built up from individual chip modules, which are interconnected by HPLC-capillaries. Selection and combination according to the given protocol is done in an empirical way. Since all operations have to be in plug mode, microdroplets need to be large enough to seal a given channel completely. In general, reliable transport of sample segments depends on nearly ideal wetting of the separation fluid to the microchannel wall and nearly ideal non-wetting conditions for the sample fluid. For aqueous sample segments this may be realized using a lipophilic surface and a mineral oil as separation medium. Therefore, the Ideal Minimum Compartment Volume (IMCV) for plug flow was introduced [1] as a parameter, defining the volume required for plug flow. This IMCV is defined as the minimum volume which is able to seal a given channel geometry completely under ideal non-wetting conditions (contact angle of the interface between the two fluids and the channel wall equals 180°). In modular arrangements chip devices are interconnected by HPLC capillaries. Sample stacks have to be transferred through these capillaries. Widely used HPLC capillaries with an inner diameter of 0.5 mm have an IMCV of about 64 nl. With respect to this, modular systems are limited in compartment size and thus in throughput and sample density. Processing of segmented sample streams uses interface-generated forces for the manipulation of the microdroplets at functional nodes with optimized geometry and wetting conditions. The quantity of these forces depends on interface tension and curvature of the interface as given by the Young–Laplace equation (1). Miniaturization of the channel system and the

* Corresponding author.

1385-8947/$ – see front matter © 2007 Published by Elsevier B.V.
doi:10.1016/j.cej.2007.07.047

droplet volume increases the curvature of the interfaces and thus the resulting pressure drop. In conclusion, not only throughput and sample density, but also reliability of the processes benefit from miniaturization and integration. Regarding this, our work is focused on the development of integrated lab-on-a-chip devices for segmented flow based application in a model based approach, which implements self control for flow management. At present, first functional elements are reported which implement the concept of self control. Double-T-injectors have been used by Ismagilov and coworkers [2] to apply self control on the formation of stacked droplet sequences. An implementation, which uses hydrodynamic resistance for regulation of droplet traffic into two arms of a Y-shaped junction is reported by Joanicot and coworkers [3]. A first implementation of self-controlled 1:1 fusion of the droplets from two droplet sequences at a Y-junction with automatic balancing of runtime differences has been developed [4] and is applied as touchstone for the developed toolkit.

1.1. Abstraction of segmented sample streams

The general abstraction of a liquid/liquid segmented sample stream is a list of individual sample volumes with individual properties, separated by a volume of separation fluid. Sample streams are guided through pipes driven by the potential drop inside the pipe. Pipes connect functional nodes for sample processing, typically with three or more fluid ports. The network itself is controlled via its global ports, interfacing to the environment. These ports may have a fixed potential (potential constraint) or may be connected to a pump system (flow rate constraint) to become a mass source or mass drain.

Based on this abstraction the simulation toolkit is implemented as a network simulation in time, consisting of connectors and functional nodes. Both, functional nodes and connectors use programmable rules, describing their operation on segmented sample streams. All volumes are located and maintained in connectors. Functional nodes do not have a volume. The network representation is a graph [5]. Iteration is done in time steps, followed by state optimization until convergence is reached.

1.2. Potential quantities and driving forces

The pressure represents the potential quantity inside the network. Global flow is directed to the global direction of decreasing pressure. Interfaces may generate local pressure drops according to their interface tension σ, the direction of curvature dir, and the characteristic radius of curvature r_{eff} according to (1).

$$\Delta p = 2 \times \text{dir} \times \frac{\sigma}{r_{\text{eff}}} \tag{1}$$

Mass flow $\dot{m}$ generates the counterpoise to global flow by fluidic friction based resistance R_{f} of the fluids inside pipes and functional nodes according to (2).

$$p = \dot{m} \times R_{\text{f}} \tag{2}$$

The relation between mass flow and pressure drop in a pipe with a total of n segments is given by (3) as the sum of interface and volume part contribution.

$$p = \sum_{i=1}^{n} 2 \times \text{dir}_{i/(i-1)} \times \frac{\sigma_{i/(i-1)}}{r_{\text{eff}\,i/(i-1)}} + \dot{m} \times R_{\text{eff}\,i} + 2 \times \text{dir}_{i/(i+1)} \times \frac{\sigma_{i/(i+1)}}{r_{\text{eff}\,i/(i+1)}} \tag{3}$$

In general, mass flow is the result of a pressure drop, but it may become a constraint in case of the connection to a mass source or mass drain. Commonly, these are global ports of the network which connect it to the environment.

1.3. Contribution of liquid/liquid interfaces to the pressure drop

Liquid/liquid interfaces generate local pressure drops dependent on the characteristic radius of curvature r_{eff} and the interface tension σ. This pressure drop may be used to seal junctions temporarily, to stop compartment motion at strictures and to control bypass flows. That way, interface-generated forces may be used for realization of self-controlling fluidic elements [4].

The geometry of interfaces itself is the result of complex interactions between the liquids, the channel walls and the force fields, induced by the internal flow and global transport. This part focuses on the contribution of local geometry and wetting conditions. Aspects of fluid dynamics are not considered in this section.

The droplet shape is effected by the local channel geometry and the interface tensions between the individual sample liquid and the separation medium, between the sample liquid and the channel walls, and between the separation medium and the channel walls. The shape may be calculated as the result of minimization of the interface energy in the given channel geometry. For static systems with no mass flow the surface evolver [6] may be applied for calculation of interface shapes dependent on geometry and interface tensions. This software directly allows for calculation of pressure drops at interfaces. With respect to its high computation speed it seems to be the preferred computation tool to derive rules from parameter studies.

As an example the modelling of the pressure drop between separation medium and test medium during passage of a stricture inside a T-shaped junction is given in Fig. 1. The graph displays the pressure in dependency on the position of the segment in relation to a nozzle geometry.

Microchannel geometry is set up as prepared by wet etching of identical half channels in two glass substrates followed by face-to-face bonding of the two half shells (Fig. 2). This process results in microchannels, having two coplanar faces at the top and the bottom of the microchannels and side walls with a circular geometry [1]. The dimensions of the planar faces are defined by the geometry of the etch mask. The radius of the side wall equals the etch depth of the channel. The simulation has been performed for a water droplet in tetradecane and a lipophilic channel wall, realized by treatment of glass surfaces with octadecyl-trichlorosilane. The pressure drop preventing the

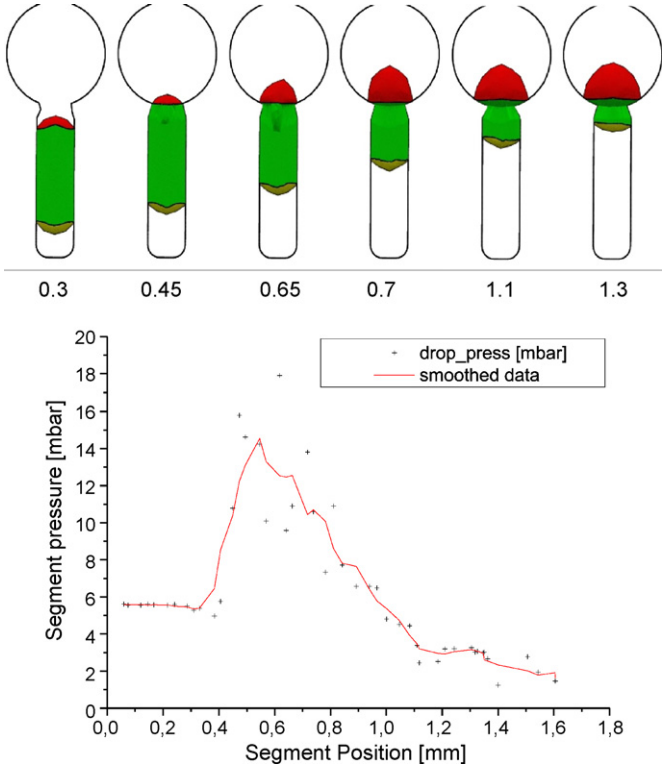

Fig. 1. Modelling of pressure drop at the liquid/liquid interface of a droplet during passage of a nozzle of a T-shaped junction into a large main channel using the surface evolver. Top: 3D views of the droplet passage through the junction along the direction of the main channel (top circle). Numbers indicate the distance of the lower interface from the lower end of the injection channel in mm. Diagram: segment internal pressure drop to the environment dependent on its position inside the microchannel. The main channel resides on environmental pressure, the injection channel is treated as a closed system without contact to the environment. Positions are given as above. Parameters: main channel geometry: mask width 10 μm, etch depth 500 μm, width 1010 μm, height 1000 μm. Injection channel geometry: mask width 140 μm, etch depth 120 μm, width 390 μm, height 240 μm. Nozzle diameter 150 μm. Interface tensions: wall/oil 3×10^{-3} N/m, wall/water 46×10^{-3} N/m, oil/water 47×10^{-3} N/m.

motion of an interface through a nozzle may be calculated and implemented as a rule.

1.4. Contribution of fluidic friction to the pressure drop

Fluidic friction results in pressure drops along the direction of flow. The quantity of the pressure drop depends on fluid dynamic parameters of the fluids itself and the characteristics of the velocity distribution inside the fluids. Each droplet volume represents a self-contained system, where no mass, but energy and impulse transfer to its local environment occur. This results in Taylor flow – a circular internal flow regime [7–10]. This flow regime considers fluidic friction between the microchannel wall and the fluid. Additionally, fluidic friction at the liquid/liquid interface contributes to the internal flow. Dependent on the friction coefficients and the relation between fluid/wall interface area and fluid/fluid interface area, the velocity of droplet motion and the channel path characteristics (curved or linear), multiple regimes of Taylor flow are observed and must be considered [11]. In addition, ultra thin films of separation medium, covering the microchannel surface may contribute to changes in the friction coefficient of the sample fluid at the microchannel walls.

Central plane flow fields for tetradecane/water two phase flows in lipophilic microchannelspresented here (Fig. 3) are measured using a special extension to μ-Particle Image Velocimetry (μPIV) [11]. In small, aqueous segments, enclosed by large segments of tetradecane internal flow is dominated by fluid/fluid friction. Maximum velocity is observed at the liquid/liquid interface. During translation in linear microchannels two vortices are observed. In curved channels the influence of the different radial velocity results in complex flow fields with a total of four vortices. In longish compartments we observe a total of about six vortices [11]. In general, all flow fields are strongly influenced by friction at the liquid/liquid interfaces. Only in longish aqueous slugs, we find a central region with liquid/wall friction influenced flow. Results from CFD simulations are in accordance with these data [11].

Regarding this diversity of flow characteristics, it will become complicated to derive rules which correctly describe the pressure distribution along a sequence of segments for a given set of process parameters. Rules must be derived either from simulations or from experimental data.

Numerical approaches use the Navier-Stokes equation to solve these problems for particular setups. CFD codes are available to run these analyses for regions limited in size and complexity [4,12]. Application of CFD to large system simulations are actually not suitable with respect to the huge computation effort for such simulations. Parameter studies may be applied to derive rules, which describe the pressure drop dependent on the related parameters for a particular subsystem. Analytical solutions of the Navier Stokese equations for laminar flow in tubes or slits, can only be applied on fluid fractions

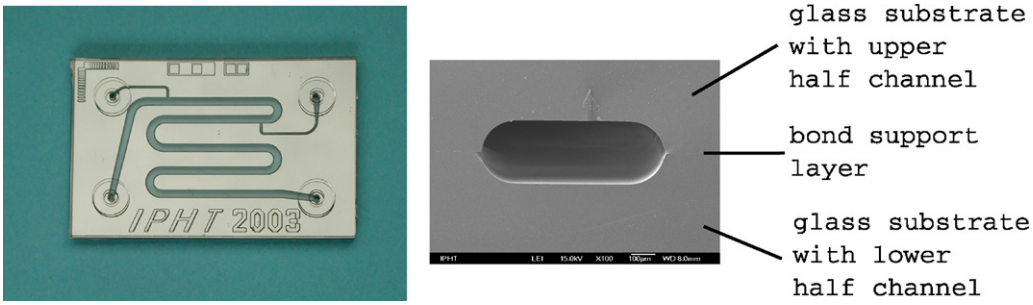

Fig. 2. Left part: micrograph of an all-glass double injector device (dimension: 16 mm × 25 mm). Right part: Raster electron micrograph of the crossection of an all-glass microchannel prepared by isotropic wet etching of glass followed by face to face bonding of two half shells.

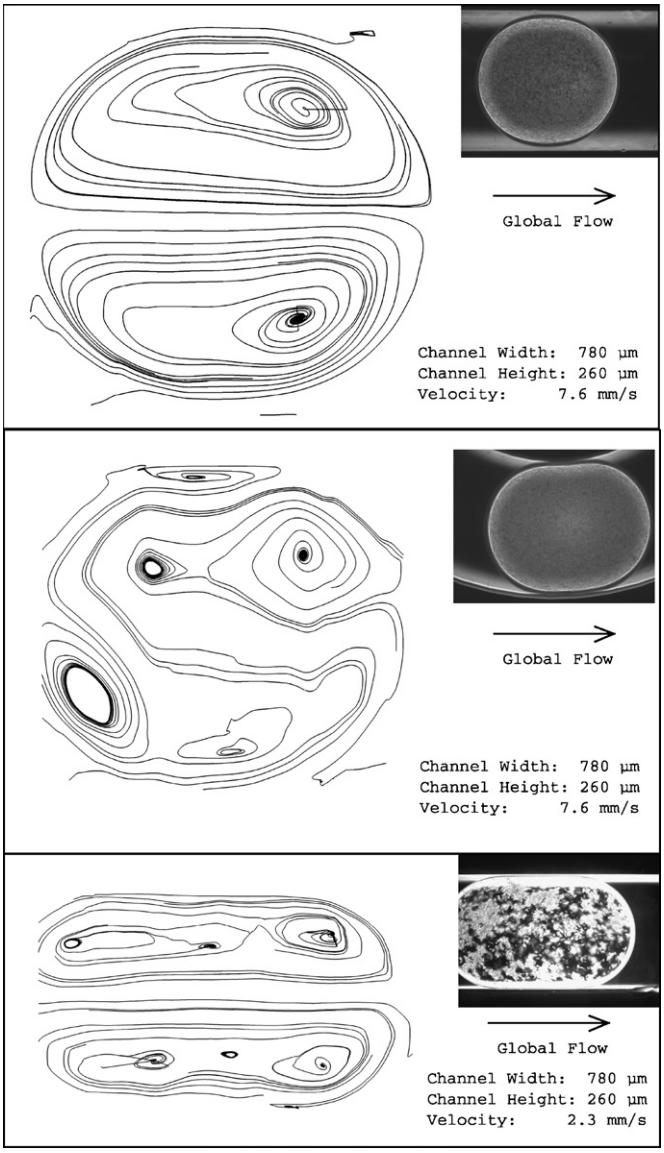

Fig. 3. Streamline representation of phase internal flow in aqueous droplets, flanked by segments of tetradecane in a lipophilic microchannel. Z-Posision is adjusted to the central plane of the microchannel. Depth of focus is about 100 µm. Top: small droplet, transported in a linear channel. Center: small droplet transported through a winding channel. Bottom: longish droplet, transported in a linear channel section.

that are distant from interfaces. Interfaces and adjacent volume fractions require a separate description [10]. Approaches are reported for the calculation of pressure fields from µPIV data for single phase flows [13]. Therefore, the pressure Poisson equation was solved using velocity data from µPIV measurement. Application to µPIV data from two phase flows may become a tool for calculation of fluid dynamic parameters of segmented sample streams.

2. Implementation details

2.1. The simulation network

The network simulation was implemented in an object oriented approach as a C++ class library using techniques of polymorphism, inheritance and virtual methods (Fig. 4). Base class for all derived classes is the class *Node*. It provides prototypes for all methods, required for the calculation. Rules, describing the behaviour of a particular class, may override methods of their parent class.

Derived from *Node* are the *Transporter*, *Distributor*, *IONode* and *Network* classes. *Transporters* have two fluid ports. Only *Transporters* and their child classes are able to store a volume. They may be aggregated to Paths. *IONodes* connect the network to the environment and serve as source or drain of mass flow. *Distributors* are functional nodes, which process and distribute sample streams. Typically, they have three fluid ports and do not have a volume. Arrangements of functional nodes with more than three ports may be set up as an aggregation of *Distributors*. Thus, *Distributors*, having more than three ports are not required. The class *Network*, which itself represents the network as a *Node*, administers the *Node* objects, aggregates *Transporters* to *Paths* and performs the network calculation. The Network itself is represented by a Graph.

Ports of functional nodes (*Distributor*, *IONode* or (sub) *Network*) are connected by a *Path* (Aggregation of transporters). All volumes are contained in *Paths*. Matrix representations of graphs [5] were applied for administration of connectivity, pressure and mass flow. Connectivity information is maintained in the C-Matrix (Fig. 5). Each column represents a *Path* and each entry in the column represents one port of a functional node, connected via the *Path*. Each column in a C-Matrix has exactly two non zero entries, which may be 1 or −1, representing the two ports of the *Path*. The sign of the entry determines the direction of the connected *Path*. A functional *Node* is represented by a matrix row. The number of entries in a row corresponds to the number of ports, provided by the functional *Node*. The pressure at the ports and the mass flow through ports are stored in adequate matrix representations called P-Matrix (pressure) and I-Matrix (Flow) at the same positions as in the C-Matrix. For incompressible media the system is in equilibrium if the law of mass conservation is satisfied in the local and global contexts. Applied to the matrix representation this occurs if all of the following conditions are satisfied.

- the sum of mass flows along a column equals zero,
- the sum along a row equals to zero or is equal to the mass flow provided by a mass source or mass drain,
- the total sum of mass flows equals zero.

That way, starting points for calculation and routes for their progression are identified as nodes of maximum inconsistency. The network calculation itself is iterative. One iteration includes the steps of network state analysis, identification of the most important focus of calculation and the route on which the focus of calculation proceeds, recalculation and validation along the route of calculation. The iteration stops when all convergence criteria are satisfied.

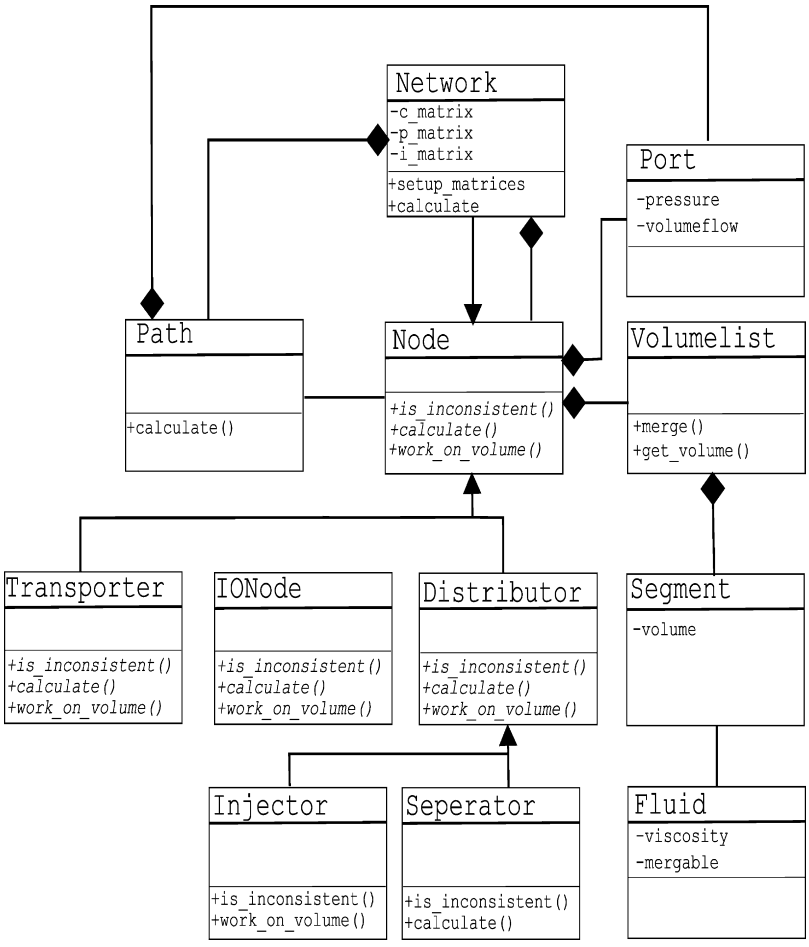

Fig. 4. Class diagram of the implemented network simulation toolkit.

2.2. Treatment of reagents and compartment sequences

Droplet sequences are handled as double linked lists of *Segments* and are attributes of volume carrying nodes, e.g. Transporters. The geometric position with respect to the start or end point of a list is calculated from the cumulative volume of the preceding or subsequent volumes and the inner volume of the transporters. Each *Segment* of the list has a mixable attribute, which describes, whether it is mixable with separation fluid or with sample fluid. In order to transfer a sub volume of a compartment between lists the sub volume has to be separated into two parts, one of them is transferred to the next list. After that a valid list is created by combining adjacent mixable volume elements.

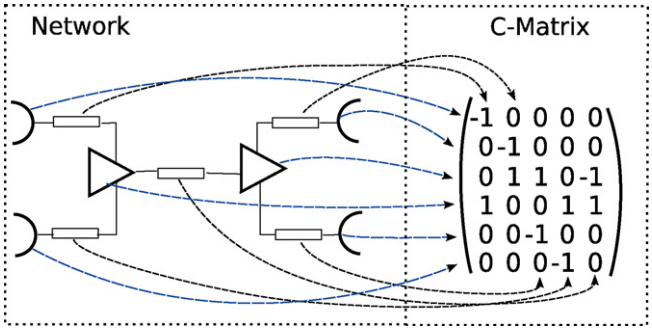

Fig. 5. Matrix representation of the network graph. Left: network representation, consisting of *IONodes* (half circle), *Paths* (rectangle) and *Distributors* (triangle). Right: Connectivity matrix.

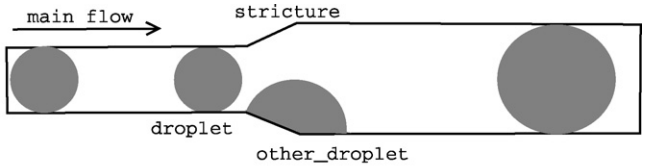


```
/* pseudo code for droplet motion */

Compartment droplet, other_droplet;
Tube  tube;
Position x;

/* Two compartments are in contact */
if( compartments_may_merge(droplet, other_droplet){
    droplet=droplet.merge_with(other_droplet);
}

if( droplet.volume()  > tube.IMCV(x)){
    enable_motion(droplet);
}
else {
    disable_motion(droplet);
}
```

Fig. 6. Pseudocode for analysis of a droplet motion capabilities at position *x*.

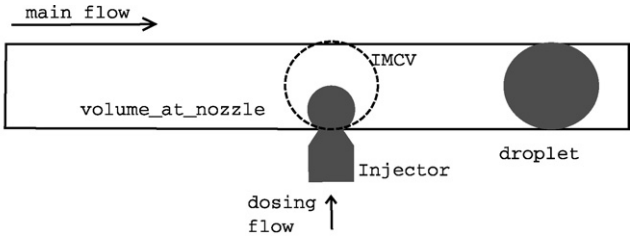


```
/* Pseudocode for segment generation at a nozzle */

Volume volume_at_nozzle;
Compartment droplet;

if( volume_at_nozzle >= IMCV) {
    New Compartment droplet(volume_at_nozzle);
    droplet.tear_off();
}
else {
  /* no_tear_off */;
   continue;
}
```

Fig. 7. Pseudocode for segment generation at a T-shaped injector with integrated nozzle.

The composition of a fluid may change in time due to an internal chemical reaction, during fusion with other fluid elements and as a result of dosing operations. This is handled by the *Segment* class, which provides methods for storing and retrieving physical and chemical properties of the fluid inside a particular segment.

2.2.1. Rules describing fundamental functional nodes

Main objectives of the present work have been the development and evaluation of a software architecture for system simulations of segmented flow based microfluidic networks. Rules describing the behaviour of functional nodes have been implemented at a high level of abstraction and simplification. Thus, recent simulations cannot provide numerically correct results, but qualitative results, which may be compared with experimental data and results of CFD simulation. Main aim of the current work was to demonstrate the ability of the developed system to handle complex architectures correctly. This is

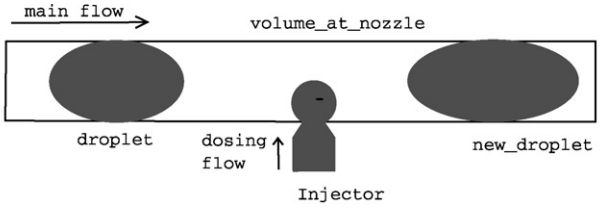


```
/* pseudocode for dosing of liquid into droplets */

Compartment droplet, new_droplet;
Volume volume_at_nozzle;

if(compartment_reaches_nozzle(droplet){
    volume_at_nozzle += droplet.volume();
    Delete droplet;
}
if(volume_at_nozzle < IMCV){
    no_tear_off(volume_at_nozzle);
}
else {
    New Compartment new_droplet=tear_off(volume_at_nozzle);
}
```

Fig. 8. Pseudocode, describing the dosing of liquids into compartments.

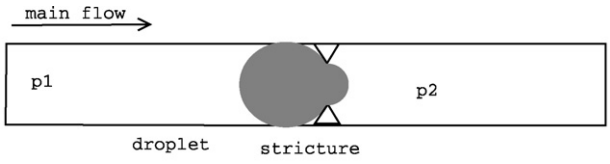


```
/* Pseudocode for stopping a compartment at a stricture */

Pressure    env_pressure_drop= p1-p2;
Compartment droplet;
Strictur    stricture;

if( env_pressure_drop >
       droplet.max_pressure_drop_at_stricture(stricture))
{
     droplet.enable_motion();
}
else
{
    droplet.disable motion();
}
```

Fig. 9. Pseudocode, describing the stopping of a compartment at a stricture.

demonstrated for the self-controlled 1:1 fusion of two segment streams. Rules discussed here are implemented in virtual methods of classes that are used in this simulation and additional test cases.

2.3. Simplifications

Main aims of this work are the evaluation of the network model and the interoperability of the functional nodes. Therefore, strong simplifications have been applied to the base classes and their virtual methods. Basic methods, implemented in the base classes use the Hagen–Poiseuille flow in tubes with a circular cross section for calculations of fluid dynamic parameters. Special flow characteristics at liquid/liquid interfaces and their adjacent regions are not considered in the base classes. This is overridden by derived classes and implemented in the rules, describing the behaviour of a particular functional node. Microchannels are assumed to have a geometry as given in Fig. 2. They provide ideal wetting conditions to the separation fluid and ideal non-wetting conditions to the sample fluid. This enables the application of IMCV based rules.

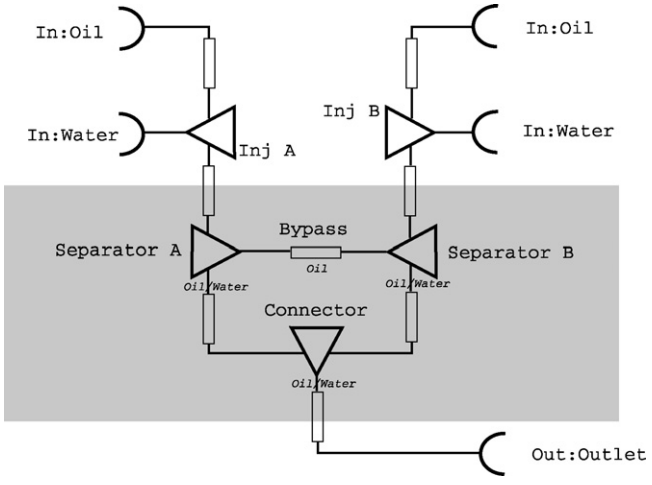

Fig. 10. Graphic representation of the network model for self controlled 1:1 fusion of two independent generated segment streams.

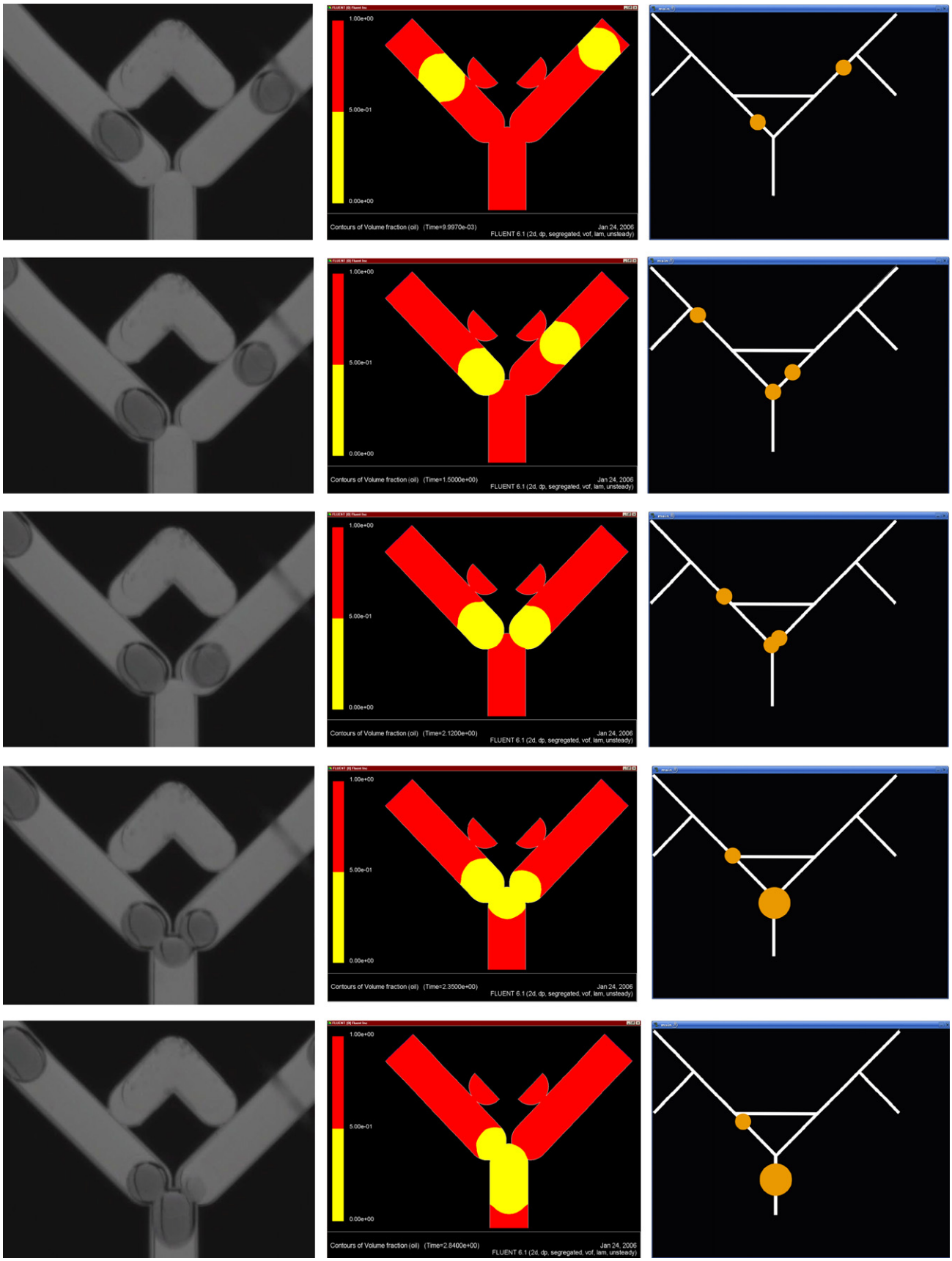

Fig. 11. Comparison of experimental data (left column), CFD Model (Fluent, 2D) (middle column) and network simulation for the self controlled 1:1 segment fusion (right column). First row: the first segment passes the bypass. Second row: it arrives and stops at the stricture. Third row: separation medium flow is guided trough the bypass until the droplet coming from the right branch arrives. Fourth row: fusion occurs and fifth row: the merged droplet leaves the junction.

2.4. Fluid pipes

Fluid pipes are used to transfer segment streams and are derived from *Connectors*. They may have variable diameters along their length and thus the IMCV depends on the position. Segments may be transported as long as their volume exceeds the IMCV. Smaller segments are settling on the channel wall and are bypassed by separation medium until another segment reaches the position. Then the segments merge and the new segment is transported if its volume exceeds the IMCV. Pseudocode is given in Fig. 6.

2.5. Injectors for segment generation

Injectors are well investigated functional elements for segment generation. Different kinds of T-shaped injectors have been reported. Mathematical models for T-shaped injectors with a rectangular channel geometry and a full height junction without a nozzle have been developed [14,15]. Injector structures with integrated nozzles in microchannels with rounded edges have been the subject to our studies [1]. T-shaped injectors, equipped with a single nozzle, have been identified as the most reliable systems for generation of small droplets with good uniformity in size and rate of droplet formation. The energy required for the tear-off of a droplet from its nozzle may be estimated as the energy required to generate twice the interface area of the nozzle [1]. Energy is introduced by fluidic friction of the separation medium passing the interface of the growing droplet which forms a stricture, and by the pressure drop along this stricture [15]. For T-shaped injectors with a single nozzle at the junction this condition is satisfied as soon as the droplet completely seals the main channel for a wide range of flow rates [1]. Thus, the IMCV of the microchannel may be used as a criterion for droplet generation. The resulting pseudo code for T-shaped injectors with integrated nozzles is given in Fig. 7.

2.6. Injectors for dosing of liquid into segments

Injectors for dosing liquids into segments are identically to the previous injectors. Dosing is realized by continual flow out of the nozzle. The volume of the droplet, settling at the nozzle inside the main channel grows until a compartment reaches its position. In this case the droplets merge and tear-off occurs (since the acceptor compartment must have at least the IMCV in order to be transported in the channel). If no compartment passes until the volume at the nozzle becomes larger than the IMCV it tears off and forms an inserted compartment. The pseudocode representation of this rule is given in Fig. 8.

2.7. Stopping a compartment at a stricture

At a stricture a segment generates a pressure drop as the result of the smaller characteristic radius of curvature r_{eff} inside the stricture. The maximum pressure drop equals to the Laplace pressure and may be calculated according to (1). The droplet stops until the pressure drop between the adjacent separation medium complements the first pressure. Pseudocode is given in Fig. 9.

3. Results

Touchstone of the network simulation toolkit is its ability to handle complex network architectures with integrated fluidic loops correctly. As the main challenge network setups with circular arrangments of functional nodes have been identified. In this case small, interface-generated forces decisively contribute to the flow directions inside the loop. Additionally, the initialization for the calculation of these structures is complicated because under-determined situations may occur. These setups are handled correctly by the present implementation. As an example serves the self controlled 1:1 fusion of the segments of two droplet sequences with self controlled balancing of runtime differences [4]. The network representation is given in Fig. 10.

The system consists of two injector structures for independent generation of two segment streams and an arrangement for self controlled 1:1 fusion of the two generated sample stacks (grey highlighted region). A constant inflow is applied at the inlets for oil and water, the outlet is set to constant pressure. The core of the system is a circular arrangement of three functional nodes. Separators implement a media selection and allow only the flow of separation medium into the bypass channel.

Inflow of water is suppressed by a stricture. The connector forms strictures to both of the inlets and a widening to the outlet. That way, the droplet, first reaching the connector stops at the stricture. The pressure drop generated by the droplet guides the flow of mineral oil through the bypass to the opposite branch of the system. Flow through the opposite branch continues until a droplet from this branch reaches the connector. Now both droplets merge in a 1:1 level and the resultant droplet is emitted from the structure.

The model was set up using the media, geometries and operation conditions as reported [4]. Fig. 11 shows the comparison of the results of CFD Model, experimental data and the results obtained from modelling the system using the developed toolkit and methods, derived from the described rules. The observed functionality is correctly modelled by the developed computational toolkit. Compared to the 2D-CFD simulation performed with FLUENT, which runs about 14 days on a Dual CPU PC machine, the network simulation of the developed system takes only 20 min. That way, it provides acceptable computing speed for the application of the toolkit for interactive optimization of fluidic networks according to a given process protocol and may be applied on the model based design and optimization of segmented flow based lab-on-a-chip systems for particular process protocols.

4. Conclusion

A toolkit for system simulations of segmented flow based microfluidic networks in time has been designed and successfully applied on the modelling of self synchronized 1:1 fusion of droplet sequences. The developed simulation network aggregates functional nodes, interconnected by virtual connectors.

Connectivity and network state are managed in special matrix representations of the network graph. Droplet sequences and reagent properties are handled as doubly linked lists. For each time step the network iterates, until convergence is reached. The toolkit models the system behaviour based on the functionality of the integrated nodes.

Functionality of nodes may be introduced and overridden by user programmable rules, which may be derived from experimental data and parameter studies of CFD models of a particular node. System simulations are only required for validation or verification of the simulation results of the toolkit. At present, the functionality is implemented on a high level of abstraction and simplification. Regarding this, the system is able to model the behaviour of complicated systems correctly. In contrast to the majority of reviewed [12] approaches the toolkit does not implement the concept of finite element calculations. The calculation region is handled as a graph representation of nodes, which themselves provide rules, describing their function on segmented sample streams and providing informations on local pressure drop and mass flow, dependent on the parameters of the direct environment. Main aim of future work is the derivation and implementation of rules, describing numerically exact the behaviour of functional nodes dependent on material constants, geometric properties and process parameters from experimental data and parameter studies of CFD models.

Acknowledgement

This work was kindly supported by the German Federal Ministry of Education and Research BMBF under reference FKZ 16SV1998 and the Thuringia Ministry of Economy, Technology and Employment under reference B 30 902 007.

References

[1] T. Henkel, T. Bermig, M. Kielpinski, A. Grodrian, J. Metze, J.M. Köhler, Chip modules for generation and manipulation of fluid segments for micro serial flow processes, Chem. Eng. J. 101 (2004) 430–445.

[2] B. Zheng, J.D. Tice, R.F. Ismagilov, Formation of droplets of alternating composition in microfluidic channels and applications to indexing of concentrations in droplet-based assays, Anal. Chem. 76 (2004) 4977–4982.

[3] G. Cristobal, J.-P. Benoit, M. Joanicot, A. Ajdari, Microfluidic bypass for efficient passive regulation of droplet traffic at a junction, Appl. Phys. Lett. 89 (2006) 034104.

[4] M. Kielpinski, D. Malsch, G. Mayer, J. Albert, J. Felbel, T. Henkel. Self controlled droplet fusion of segmented sample streams. International Conference on Micro Reaction Technology IMRET 9, Potsdam 6.9.2006–8.9.2006.

[5] J. W. Harris, H. Stocker, Representation of graphs, in: Handbook of Mathematics and Computational Science, Springer, 1998, p. 485, ISBN 98-20290.

[6] K. Brakke, The surface evolver, Exp. Math. 1 (1992) 141–165.

[7] H. Liu, Ch.O. Vandu, R. Krishna, Hydrodynamics of Taylor flow in vertical capillaries: flow regimes, bubble rise, velocity, liquid slug length, and pressure drop, Ind. Eng. Chem. Res. 44 (2005)4884–4897.

[8] A. Günther, M. Jhunjhunwala, M. Thalmann, M.A. Schmidt, K.F. Jensen, Micromixing of miscible liquids in segmented gas/liquid flow, Langmuir 21 (2005) 1547–1555.

[9] J.D. Tice, H. Song, A.D. Lyon, R.F. Ismagilov, Formation of droplets and mixing in multiphase microfluidics at low values of the Reynolds and the capillary numbers, Langmuir 19 (2003) 9127–9133.

[10] M.N. Kashid, I. Gerlach, S. Goetz, J. Franzke, J.F. Acker, F. Platte, D.W. Agar, S. Turek, Internal circulation within the liquid slugs of a liquid–liquid slug-flow capillary microreactor, Ind. Eng. Chem. Res. 44 (2005) 5003–5010.

[11] D. Malsch, M. Kielpinski, R. Merthan, J. Albert, G. Mayer, J. M. Köhler, H. Süße, M. Stahl, T. Henkel. μPIV-Analysis of Taylor Flow in Microchannels, Presentation on International Conference on Micro Reaction Technology IMRET 9, Potsdam 6.9.2006–8.9.2006, submitted for publication in Chem. Eng. J.

[12] D. Erickson, Towards numerical prototyping of labs-on-chip: modeling for integrated microfluidic devices, Microfluidics Nanofluidics 1 (2005) 301–318.

[13] N. Fujisawa, Y. Nakamura, F. Matsuura, Y. Sato, Pressure field evaluation in microchannel junction flows through μ-PIV measurement, Microfluidics Nanofluidics (2006) ISSN: 1613-4982 (Paper) 1613-4990 (Online), DOI: 10.1007/s 10404-006-0088-5, Issue: Online First, Published online: 31 March 2006.

[14] S. van der Graaf, T. Nisisako, C.G.P.H. Schroen, R.G.M. Van der Sman, R.M. Boom, Lattice Boltzmann simulations of droplet formation in a T-shaped microchannel, Langmuir 22 (2006) 4144–4152.

[15] P. Garstecki, M.J. Fuerstmann, H.A. Stone, G.M. Whitesides, Formation of droplets and bubbles in a microfluidic T-Junction – scaling and mechanism of break up, Lab Chip 6 (2006), pp. 437–446.